Bioresource Technology 211 (2016) 327–338

Contents lists available at ScienceDirect

Bioresource Technology

journal homepage: www.elsevier.com/locate/biortech

Autotrophic growth and lipid production of *Chlorella sorokiniana* in lab batch and BIOCOIL photobioreactors: Experiments and modeling

Alessandro Concas [a,*], Veronica Malavasi [b], Cristina Costelli [b], Paolo Fadda [b], Massimo Pisu [a], Giacomo Cao [b,c]

[a] Center for Advanced Studies, Research and Development in Sardinia (CRS4), Loc. Piscina Manna, Building 1, 09010 Pula (CA), Italy
[b] Interdepartmental Center of Environmental Science and Engineering (CINSA), University of Cagliari, Via San Giorgio 12, 09124 Cagliari, Italy
[c] Department of Mechanical, Chemical and Materials Engineering, University of Cagliari, Piazza d'Armi, 09123 Cagliari, Italy

HIGHLIGHTS

- A mathematical model to evaluate lipid productivity of *C. sorokiniana* is proposed.
- Experiments were performed in batch lab-scale and BIOCOIL photobioreactors.
- Quite good lipid productivity and FAMEs composition was attained with the BIOCOIL.
- Experimental data have been successfully predicted through the proposed model.
- The model allows optimizing the fed-batch operation of the BIOCOIL.

ARTICLE INFO

Article history:
Received 15 January 2016
Received in revised form 15 March 2016
Accepted 16 March 2016
Available online 18 March 2016

Keywords:
C. sorokiniana
BIOCOIL photobioreactor
Mathematical modeling
FAMEs
Lipid productivity

ABSTRACT

A novel mathematical model for the quantitative assessment of the effect of dissolved nitrogen on the autotrophic batch-growth and lipid accumulation of *Chlorella sorokiniana*, is proposed in this work. Model results have been validated through comparison with suitable experimental data performed in lab photobioreactors. Further experiments have been then performed using the BIOCOIL photobioreactor operated in fed-batch mode. The experimental results, which show that a maximum growth rate of 0.52 day^{-1} and a lipid content equal to 25 %wt can be achieved with the BIOICOIL, have been successfully predicted through the proposed model. Therefore, the model might represent a first step toward the development of a tool for the scale-up and optimization of the operating conditions of BIOCOIL photobioreactors. Finally, the fatty acid methyl esters obtained by trans-esterification of lipids extracted from *C. sorokiniana*, have been analyzed in view of the assessment of their usability for producing biodiesel.

1. Introduction

It is well recognized that microalgae represent today one of the most promising renewable feedstocks for the production of a wide range of consumer goods such as biofuels, nutraceuticals, pharmaceuticals, bioplastics, functional food, lubricants and food for aquaculture systems. However, the current technology, based on the exploitation of closed photobioreactors (PBRS), should be properly optimized, in order to become economically sustainable. In particular, lipid productivity of microalgae should be increased with respect to the values achieved so far. Several methods are currently being investigated for boosting lipid biosynthesis in microalgae. Aside the ones based on the exploitation of genetic engineering tools, all these techniques have in common process conditions that lead the microalgae to face stress conditions which trigger lipid synthesis. Specifically, techniques exploiting extreme pH and temperature conditions, high radiation, osmotic stress, and high heavy metals concentration, are currently under investigation (Sharma et al., 2012). While some of these methods are able to increase the lipid content of microalgae, most of them result in a significant lowering of the biomass productivity which, in turn, cancels out the positive effect deriving from augmented lipid content.

Although it still poses concerns of reduced biomass productivity, the induction of nitrogen starvation in the culture seems to be the only feasible technique for boosting lipid productivity on

* Corresponding author.
E-mail address: aconcas@crs4.it (A. Concas).

http://dx.doi.org/10.1016/j.biortech.2016.03.089
0960-8524/

Notations

C_b	concentration of total microalgal biomass ($g_{dw}\ m^{-3}$)
C_f	concentration of the fatty acid fraction of algal biomass ($g_{Fe}\ m^{-3}$)
C_ℓ	concentration of the lipidic fraction of algal biomass ($g_{dw}\ m^{-3}$)
C_N	total mass concentration of N species in bulk phase ($g_N\ m^{-3}$)
C_x	concentration of functional fraction of algal biomass ($g_{dw}\ m^{-3}$)
I_0	incident light intensity ($\mu E\ m^{-2}\ min^{-1}$)
D	dilution ratio (min^{-1})
I_{av}	average light intensity within the culture ($\mu E\ m^{-2}\ min^{-1}$)
k_d	mass loss of the functional fraction of microalgae (min^{-1})
$k_{f\to\ell}$	rate constant for the conversion of fatty acids to lipids (min^{-1})
K_N	half saturation constant of nitrogen ($g_N\ m^{-3}$)
MW_N	molecular weight of nitrogen ($g_N\ mol_N^{-1}$)
P	carbon-specific photosynthetic rate (net carbon fixation rate) ($g_C\ g_{dw}^{-1}\ min^{-1}$)
P_c^{max}	carbon-specific maximum photosynthetic rate ($g_C\ g_{dw}^{-1}\ min^{-1}$)
P_c^{sat}	carbon-specific light-saturated photosynthetic rate ($g_C\ g_{dw}^{-1}\ min^{-1}$)
q_{Chla}	chlorophyll-a cell quota ($g_{Chla}\ g_{dw}^{-1}$)
q_ℓ	lipid cell quota ($g_{dw}\ g_{dw}^{-1}$)
q_ℓ^{max}	maximum lipid quota of microalgae ($g_{dw}\ g_{dw}^{-1}$)
q_N	nitrogen cell quota ($g_N\ g_{dw}^{-1}$)
Q_N^{max}	maximum nitrogen cell quota above which nitrogen uptake is stopped ($g_N\ g_{dw}^{-1}$)
Q_N^{min}	minimum nitrogen cell quota under which growth is inhibited ($g_N\ g_{dw}^{-1}$)
v_N	nitrogen uptake rate ($g_N\ g_{dw}^{-1}\ min^{-1}$)
v_N^{max}	maximum nitrogen uptake rate ($g_N\ g_{dw}^{-1}\ min^{-1}$)
R	radius of photobioreactors or of the tube of BIOCOIL (m)

Greek letters

α	optical cross section of chlorophyll-a ($m^2\ g_{Chla}^{-1}$)
$\gamma_{c/x}$	average carbon content of the functional fraction of microalgae ($g_C\ g_{dw}^{-1}$)
$\gamma_{c/f}$	average carbon content of the fatty acid fraction of microalgae ($g_C\ g_{dw}^{-1}$)
μ	specific growth rate of the non-lipid fraction of microalgae (min^{-1})
μ_{max}	maximum specific growth rate of the non-lipid fraction of microalgae (min^{-1})
θ_{Chla}^N	weight of chloropyll synthesized for unit weight of nitrogen assimilated ($g_{Chla}\ g_N^{-1}$)
$\theta_{Chla}^{N,max}$	maximum chloropyll synthesized for unit weight of nitrogen assimilated ($g_{Chla}\ g_N^{-1}$)
τ_a	optical extinction coefficient for biomass ($m^2\ g^{-1}$)
ω	angle of incidence of light (rad)
$\Gamma_{f\to\ell}$	rate constant for the conversion of fatty acids to lipids ($g\ m^{-3}\ min^{-1}$)
Φ	quantum efficiency of photosynthesis ($g_C\ \mu E^{-1}$)
Π	volumetric productivity ($g_{dw}\ m^{-3}\ min^{-1}$)

Superscripts

0	initial value
f	final value
max	maximum value
min	minimum value
sat	saturation value
tot	total value

Subscripts

b	total biomass which accounts both lipid and non-lipid fraction
c	carbon specific value
Chla	chlorophyll-a
f	fatty acid fraction of biomass
$f\to\ell$	conversion of fatty acids to lipids
ℓ	lipid fraction of biomass
x	functional fraction of biomass

the large scale in an economically sustainable fashion (Concas et al., 2014b; Sharma et al., 2012). Indeed, under nitrogen starvation, biomass growth and photosynthesis become decoupled and, while protein synthesis is interrupted due to the unavailability of nitrogen, carbon internalization continues due to the photosynthetic mechanism. This leads to the unbalancing of carbon and nitrogen content within the cell which, as a response, activates specific metabolic processes aimed to store the excess carbon into high energy molecules such as lipids. However, as for the techniques based on the induction of stress conditions, although the lipid content is augmented, the growth rate decreases correspondingly and thus the resulting lipid productivity is similar to the one which might be obtained by cultivating microalgae under normal conditions. Hence, since the increase of lipid productivity is the target of the nitrogen starvation strategy, it is apparent that the identification of the trade-off value of nitrogen concentration is a key issue in view of the implementation of this technique at the industrial scale.

For these reasons, further and deeper investigations about the effect of nitrogen depletion on lipid productivity are required especially for strategic microalgal strains such as *Chlorella sorokiniana*. Despite the fact that, the latter one is a very promising strain in view of producing biofuels (Kobayashi et al., 2015), only few papers have been so far devoted to the systematic investigation of the effect of nitrogen starvation on the lipid productivity and quality of *C. sorokiniana*, especially when grown under photoautotrophic conditions. In fact, most of the work refers to mixotrophic and/or heterotrophic conditions (Kobayashi et al., 2015; Orsini et al., 2016a,b).

The most recent and comprehensive study available in the literature about the effect of nitrogen starvation on the photoautotrophic growth and lipid accumulation of *C. sorokiniana* is the one by Negi et al. (2015). In this work, by assessing growth, photosynthesis and respiration rates as well as the chlorophyll and lipid content dynamics of *C. sorokiniana*, it was demonstrated that this strain is capable to achieve high lipid productivities even when grown under N-limiting conditions. These results confirm that the N-starvation strategy might be adopted at the industrial scale to boost lipid productivity of microalgae. In spite of the relevance of these results, no quantitative and exhaustive explanation about how nitrogen can influence the lipid biosynthesis in *C. sorokiniana* under photoautotrophic conditions, has been so far provided. In particular, no mathematical models capable to describe the effect of nitrogen starvation on the photoautotrophic growth and lipid accumulation of *C. sorokiniana* has been so far proposed. Such a lack, which is common to most of the studies available in the

literature, represents one among the different causes which have limited the exploitation of the nitrogen starvation strategy to improve bio-oil yields of *C. sorokiniana* at the large scale.

Consequently, the goal of the present work is to propose a complete mathematical model to quantitatively describe the growth of *C. sorokiniana* and its capability to accumulate lipid in response to nitrogen starvation operating conditions. In order to validate model results, specific experiments in batch photobioreactors have been performed using this strain while the dissolved nitrogen concentration was changed. In these experiments, particular attention has been devoted to the assessment of the effect of nitrogen concentrations on the final quality of FAMEs (Fatty Acid Methyl Esters) obtained by transesterification of lipids. In fact, the latter one is a critical parameter for the sustainable application of the microalgae technology to the large scale (Klofutar et al., 2010; Likozar and Levec, 2014; Šoštarič et al., 2012). Finally, once the optimal nitrogen concentration identified, the possibility to scale-up the investigated process in a BIOCOIL photobioreactor has been evaluated, for the first time, with *C. sorokiniana*. The obtained experimental results, which confirmed the possibility to exploit *C. sorokiniana* in a productive framework, have been suitably predicted through the proposed model.

2. Methods

2.1. Microorganism and culture medium

An authentic fresh water strain Chlorella sorokiniana was obtained from Sammlung von Algenkulturen at the University of Göttingen (SAG 211-8k) and then investigated in this work. Stock cultures were propagated and maintained under axenic conditions in Erlenmeyer flasks with a Bold's basal medium (BBM), whose composition is shown in the Supplementary material, under incubation conditions of 25 °C, a photon flux density of 98 $\mu E\ m^{-2}\ s^{-1}$ provided by four 15 W white fluorescent tubes, and a light/dark photoperiod of 12 h. Flasks were incubated in an orbital shaker and continuously shaken at 65 rpm.

2.2. Culture medium

The BBM growth medium was used for the cultivation of *C. sorokiniana* in the base case batch experiment. The initial concentration of nitrogen in the BBM medium, hereafter indicated by the symbol C_N^0, was equal to 41.6 $g_N m^{-3}$ corresponding to 250 $g_{NaNO_3} m^{-3}$. However, the latter one was varied in the framework of suitable experiments performed with the aim of assessing the effect of nitrogen starvation on lipid productivity of *C. sorokiniana*. Specifically, the effects arising from the reduction by one-fifth (1/5N-BBM) and the increase by five times (5N-BBM), respectively the initial nitrogen concentration, were investigated. The growth medium used during the experiments in the BIOCOIL was the standard BBM specified above.

2.3. Culture conditions

Batch growth experiments were performed in 1 L Pyrex bottles under axenic conditions. During cultivation, the culture was agitated at 300 rpm using magnetic PFTE stir bars and a magnetic stirrer. The bottles and the magnetic stir bars, as well as culture media, were sterilized in autoclave at 121 °C for 20 min prior to microalgae inoculation. During cultivation, the bottles were stoppered by means of cotton plugs wrapped in cotton gauze in order to prevent external contamination while, at the same time, assuring atmospheric CO_2 diffusion within the culture. Algae were cultured at room temperature and under a photon flux density of 100 $\mu E\ m^{-2}\ s^{-1}$ provided by six 11 W white fluorescent tubes and a light/dark photoperiod of 12 h. All experiments were carried out in duplicate. Further experiments were then performed out using the BIOCOIL photobioreactor, which consisted of a 6 L helical tubular photobioreactor coupled with a degasser system, as described in the literature (Steriti et al., 2014). Briefly, the light collector of the photobioreactor consisted of 66 m transparent polyurethane tubing having a diameter of 2 cm and arranged around a circular metal frame. It was internally illuminated by three 60 W white fluorescent lamps providing a light intensity of 100 $\mu E\ m^{-2}\ s^{-1}$ for a light–dark photoperiod of 12 h. Liquid circulation in the light collector was assured by a peristaltic pump. The degasser unit was a 1 L bubble column that allowed removing photosynthetic oxygen by exposing the broth to atmosphere. Once the culture approached the stationary growth phase, the photobioreactor was operated in fed-batch mode. Specifically, after the 14th cultivation day, 800 mL of culture were daily withdrawn and then replaced by an equal volume of fresh BBM medium. The withdrawals made during the operation in fed-batch mode were then used for lipid extraction.

2.4. Biomass and pH measurement

The growth of microalgae was monitored through spectrophotometric measurements (Genesys 20 spectrophotometer, Thermo Scientific, Walthman, USA) of the culture media optical density (OD) at 663 nm wavelength (D663) with 1 cm light path. The biomass concentration C_b ($g_{dw}\ L^{-1}$) was calculated from OD measurements using a suitable C_b vs OD calibration curve, which was obtained by gravimetrically evaluating the biomass concentration of known culture medium volumes that were previously centrifuged at 4000 rpm for 15 min and dried at 105 °C for 24 h. The pH was measured daily by pH-meter (Basic 20, Crison).

2.5. Lipid colorimetric quantification

A colorimetric method recently proposed in the literature and based on the use of Sulpho-Phospho-Vanillin (SPV) was adopted to quantify the lipid content of microalgae (Mishra et al., 2014). To this aim, 0.6 g vanillin were dissolved in 10 ml absolute ethanol and then in 90 ml deionized water and stirred continuously. Subsequently 400 ml of concentrated phosphoric acid was added to the mixture. The resulting reagent was then used to perform the SPV reaction with a known amount of algal biomass suspended in a known volume (100 μl) of water. In the present work a further step, with respect to the current literature (Mishra et al., 2014), was carried out wherein the algal cells were lysed by sonication using an ultrasonic bath for 30 min before quantification. Subsequently, 2 mL of concentrated (98%) sulfuric acid was added to the sample. The resulting solution was heated for 10 min at 100 °C and then cooled for 5 min using an ice bath. Next, after the addition of 5 mL of freshly prepared phospho-vanillin reagent, the sample was incubated for 15 min at 37 °C and shaken at 200 rpm. Afterward, the absorbance at 530 nm was measured and then translated in terms of lipid content of the sample by using a calibration curve, *i.e.* $\text{lipids (mg)} = 0.209 \cdot OD_{530} + 0.017$, which was previously obtained by performing the SPV reaction with known amounts of lipid created by dissolving canola oil in chloroform according to the procedure proposed in the literature (Mishra et al., 2014).

2.6. Cell disruption, lipid extraction and fatty acid methyl esters analysis

Once the culture in the photobioreactor reached the stationary growth phase, microalgae were first harvested and then centrifuged to obtain a concentrated pellet of wet biomass. The

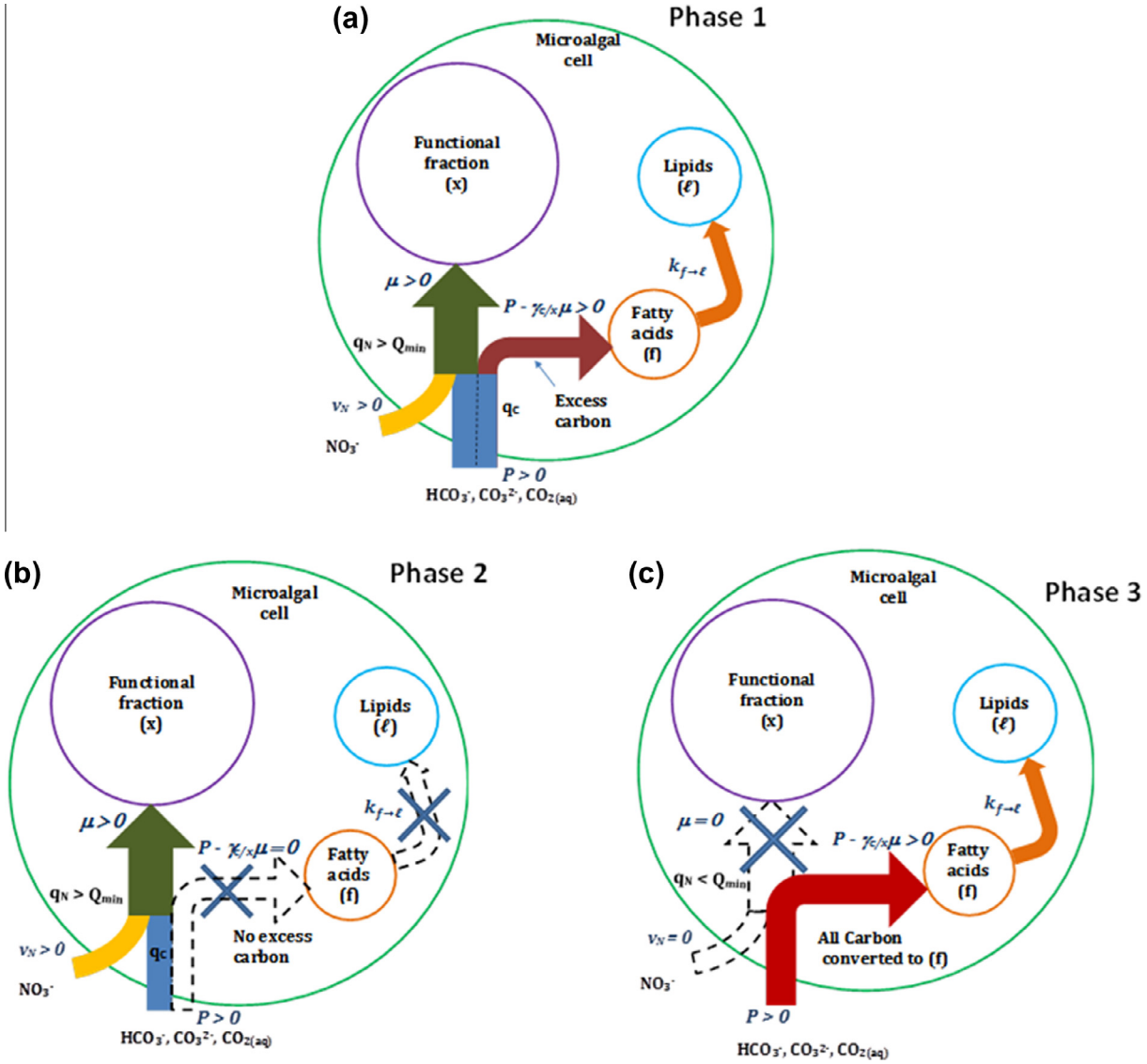

Fig. 1. Conceptual scheme of phenomena taken into account by the model: (a) The high value of photosynthetic rate P caused by the high light intensity boosts excess carbon acquisition which drives lipid synthesis, even if nitrogen is available and proteins are simultaneously synthesized; (b) The photosynthetic rate *P* decreases as a result of the increased optical density of the culture while the available nitrogen concentration is still high thus provoking the use of all the acquired carbon for the production of functional biomass; (c) The consumption of nitrogen doesn't permit the synthesis of functional material and thus all the carbon is used for the synthesis of lipids.

exact weight of dry biomass contained in the wet pellets was evaluated by means of a suitable calibration line obtained by gravimetrically evaluating the wet weight of biomass obtained after centrifugation and its corresponding dry weight after drying at 105 °C for 24 h (Steriti et al., 2014). Next, wet pellets containing known amounts of dry biomass were subjected to the cell disruption procedure, which consisted of contacting them with selected volumes of the disrupting solution within a falcon flask that was kept sealed and continuously shaken at 300 rpm at room temperature for a suitably prolonged time. The disrupting medium consisted of an aqueous solution of H_2O_2 (0.5 M). Once the desired contact time was elapsed (4 min), the disruption reaction was suddenly quenched by diluting the entire reacting mixture ten times of its original volume through the addition of ethanol (Steriti et al., 2014). Neutral lipid extraction was then performed directly on the wet disrupted biomass by taking advantage of ethanol and hexane according to a method consisting of a slight modification of a technique proposed in the literature (Fajardo et al., 2007). The percent weight of lipids extracted from the dry biomass was then evaluated as the ratio between the weight of lipid obtained and the dry weight of microalgae subjected to extraction. The composition of FAMEs, obtained by transesterification of the extracted lipids with methanol-acetyl chloride, was determined according to the European regulation EEC n° 2568 (1991). To this aim, a suitable chromatograph equipped with a flame ionization detector (FID) (Thermo Trace Ultra, GC-14B) and a RTX-WAX column T (fused silica) maintained at 180 °C was used.

3. Mathematical model

3.1. Conceptual model

According to the present model, the cell is considered to consist of three distinct compartments, i.e. the free fatty acid fraction (*f*), the lipid fraction (ℓ) and finally the functional fraction (x) which represents the bio-synthetic apparatus and is constituted by all the molecules having functions different from the energy storage

one. On the contrary, the fractions (f) and (ℓ) account for all the intracellular compounds whose role is to store the carbon (and thus energy) excess deriving from photosynthesis under nitrogen starvation. The sum of the masses of the above fractions returns the total microalgal biomass (b). Moreover, the growth of microalgae is conceptually divided into three phases wherein different phenomena rule the synthesis of functional biomass or lipids depending on the light intensity and nitrogen availability in solution (Fig. 1).

As shown in Fig. 1, during microalgae cultivation, the dissolved inorganic carbon (i.e. $CO_{2(aq)}, HCO_3^-, CO_3^{2-}$) is taken up by the cell from the bulk liquid and then used in the dark phase of photosynthesis by the Calvin's Cycle to produce glyceraldehyde 3-phosphate (q_c in the figure). The so fixed carbon is then involved in the central metabolic pathways of the cell leading to the biosynthesis of several macromolecules among which the functional ones, i.e. proteins, nucleic acids, phospholipids and carbohydrates, as well as the storage ones, i.e. fatty acids and lipids. Thus, depending on the ratio between the internal carbon and nitrogen, metabolism is shifted toward the production of functional or storage molecules. In particular, during the first days of cultivation, the low initial optical density permits a proper diffusion of light in the culture and thus photosynthesis can take place very efficiently leading to an high carbon fixation rate (cf. Fig. 1a). Furthermore, since the culture is initially nitrogen-replete, even nitrogen is absorbed from solution during this phase and thus functional biomass (x) can be synthesized by the cell through a suitable combination of the fixed carbon with the fixed nitrogen. Nevertheless, the high initial photosynthetic rate leads the internal carbon to exceed the maximum C:N stoichiometric ratio allowed to synthesize proteins. Accordingly, an excess of carbon takes place. As shown in Fig. 1a, the latter one is used by the cells for the production of fatty acids that are subsequently expelled from the chloroplast to the cytoplasm and thus elaborated in the endoplasmic reticulum to produce lipids (Mairet et al., 2011).

As cell number increases, the optical density of the culture is augmented and consequently the carbon fixation driven by photosynthesis is reduced. Therefore, at a certain point, the internal nitrogen and carbon are almost balanced, and thus the latter one is preferably used along with nitrogen to produce functional compounds, i.e. proteins, thus preventing lipid synthesis due to the unavailability of excess carbon (Fig. 1b).

Under batch conditions, as the growth process proceeds further, the nitrogen in solution is consumed and thus the corresponding intracellular concentration becomes very low. Accordingly, the minimum stoichiometric ratio N:C needed to synthesize proteins is not guaranteed anymore and thus all the carbon internalized by photosynthesis from this moment on, is used to produce fatty acids and then lipids (cf. Fig. 1c). Given the high energy density of lipids, this mechanism permits the cell also to store the energy excess, which enters the cells when the light incoming flux is too high.

An attempt to model these phenomena from the kinetic point of view was made in the literature (Mairet et al., 2011). However, the fatty acids compartment was neglected since their conversion to lipids was considered to occur very quickly. On the contrary, the present model takes separately into account the conversion of the excess carbon into fatty acids and the conversion of fatty acids into lipids. In fact, the process of conversion of fatty acids into lipids englobes the phases wherein the fatty acids are expelled from the chloroplast toward the cytoplasm, the passage from the cytoplasm to the endoplasmic reticulum, the reactions within the latter one which lead to the production of lipids and, finally, the expulsion of lipid droplets into the cytoplasm (Concas et al., 2014a). Accordingly, the assumption that the conversion of fatty acids would occur very quickly seem to be somehow unrealistic and thus the two steps depicted in Fig. 1 are considered separately in the model here proposed.

3.2. Growth and nutrient's consumption dynamics

In quantitative terms, the net carbon fixation rate $P(g_C g_{dw}^{-1} min^{-1})$ can be evaluated as a Poisson function of average light intensity $I_{av}(\mu E m^{-2} min^{-1})$ as follows (Quinn et al., 2011)):

$$P = P_C^{sat} \cdot \left[1 - \exp\left(-\frac{\alpha \cdot \Phi \cdot q_{Chla} \cdot I_{av}}{P_C^{sat}}\right)\right] \tag{1}$$

where $q_{Chla}(g_{Chl} g_{dw}^{-1})$ represents the intracellular content of chlorophyll-a and $\alpha(m^2 g_{Chl}^{-1})$ is the optical cross section of chlorophyll-a, while $\Phi(g_C \mu E^{-1})$ is the quantum efficiency of photosynthesis. The symbol P_C^{sat} represents the carbon-specific light-saturated photosynthetic rate which can be written as follows (Ward et al., 2012):

$$P_C^{sat} = P_C^{max} \cdot \left(1 - \frac{Q_N^{min}}{q_N}\right) \tag{2}$$

where $q_N(g_N g_{dw}^{-1})$ is the intracellular quota of nitrogen while $Q_N^{min}(g_N g_{dw}^{-1})$ is the minimum content of nitrogen that allows the cell to survive while the remaining symbol's significance is reported in the Notation. Depending upon the availability in solution, as well as from the intracellular content, nitrogen is continuously absorbed by the cell and used, along with the intracellular carbon, to build up functional biomass (x). Specifically, the rate of nitrogen uptake is related to the nitrogen concentration in solution and is down-regulated by a linear satiation function of the cell quota q_N as cells approach their maximum allowed content of nitrogen (Ward et al., 2012):

$$v_N = v_N^{max}\left(\frac{Q_N^{max} - q_N}{Q_N^{max} - Q_N^{min}}\right) \cdot \frac{C_N}{K_N + C_N} \tag{3}$$

where C_N is the total mass concentration of nitrogen in the bulk liquid. From Eq. (3) it can be inferred that the function expressing the cell satiation state, reported within parenthesis, is zero when the cell quota q_N is equal to its maximum allowed value Q_N^{max}, while it reaches the value 1 when q_N approaches the minimum allowed value Q_N^{min} below which no cell growth can take place. Such a function well describes the real behavior of microalgae cells which are capable to assimilate nitrogen at a rate which increases as its internal content decreases. On the other hand, when the internal quota is maximum, microalgal cells activate specific mechanisms that prevent excessive accumulation of any type of nutrient by decreasing to zero the uptake rate (Ward et al., 2012). Since the nitrogen uptake by algae leads to its consumption in the growth medium, the following mass balance can be written to describe the time evolution of its concentration in the bulk liquid phase of the batch system under investigation:

$$\frac{dC_N}{dt} = -v_N \cdot C_x \tag{4}$$

along with the corresponding initial condition:

$$C_N = C_N^0 = MW_N[NO_3^-]^0 \quad at \quad t = 0 \tag{5}$$

where C_x is the concentration of the functional fraction of algal biomass and $[NO_3^-]^0$ is the initial molar concentration of nitrates in the growth medium. On the other hand, nitrogen absorption leads the

internal nitrogen quota q_N to increase according to the following ordinary differential equations (Cherif and Loreau, 2010):

$$\frac{dq_N}{dt} = v_N - \mu \cdot q_N \tag{6}$$

along with the initial condition:

$$q_N = q_N^0 \quad at \quad t = 0 \tag{7}$$

where the product $\mu \cdot q_N (g_N g_{dw}^{-1} min^{-1})$ represents the rate at which nitrogen is consumed within the cell to produce functional proteins. The material balance for the functional fraction in batch reactors can be then written as follows (Packer et al., 2011):

$$\frac{dC_x}{dt} = (\mu - k_d) \cdot C_x \tag{8}$$

along with the corresponding initial condition:

$$C_x = C_x^0 \quad at \quad t = 0 \tag{9}$$

The specific rate $\mu(min^{-1})$ at which the functional biomass grows, can be limited either by nitrogen or by the intracellular carbon that, in the last resort, depends from light intensity. When growth occurs under nitrogen starvation conditions, the rate can be quantitatively evaluated through the well-known Droops model (Cherif and Loreau, 2010). On the contrary, when carbon (and thus light intensity) is the main limiting factor, the growth rate of microalgae can be described through the standard single-hit Poisson model of photosynthesis (Packer et al., 2011). Such model allows evaluating the specific growth rate through normalization of the net carbon fixation rate of microalgae, to the carbon content $\gamma_{c/x}$ ($g_C\ g_{dw}^{-1}$) of the functional fraction of microalgae. According to the literature the value of $\gamma_{c/x}$ is considered to remain constant during microalgal growth (Packer et al., 2011). Under these assumptions, the Liebig's Law of the minimum for describing the specific growth rate of functional fraction of microalgae can be written as follows:

$$\mu = \min\left\{\mu_{max}\left(1 - \frac{Q_N^{min}}{q_N}\right); \frac{P}{\gamma_{c/x}}\right\} \tag{10}$$

The significance of the symbols is reported in the Notation. The equation above states also that, when the intracellular nitrogen is enough, all the carbon fixed in Calvin's Cycle is used along with nitrogen for producing functional biomass (x).

3.3. Lipid accumulation dynamics

As it can be observed from Fig. 1, under nitrogen starvation conditions and if light intensity is sufficient, internal carbon is used to produce functional biomass at a rate ($\mu \cdot \gamma_{c/x}$) which is lower than that one (P) at which carbon is fixed by photosynthesis. Basically, under nitrogen starvation, carbon uptake and functional biomass growth become decoupled and, as a result, an excess of carbon is internalized with respect to the minimum amount needed to synthesize functional biomass. The carbon excess is then stored by the cells in the form of lipids through an intermediate step consisting of the synthesis of fatty acids (Mairet et al., 2011). The rate at which the excess carbon is converted into fatty acids is thus equal to $(P - \gamma_{c/x}\mu) \cdot C_x/\gamma_{c/f}$ and, accordingly, the mass balance for the fatty acids is given by:

$$\frac{dC_f}{dt} = \frac{(P - \gamma_{c/x}\mu)C_x}{\gamma_{c/f}} - \Gamma_{f\to\ell} \tag{11}$$

along with the initial condition:

$$C_f = C_f^0 \quad at \quad t = 0 \tag{12}$$

where $\gamma_{c/f}(g_C \cdot g_{dw}^{-1})$ is the average carbon content of microalgal fatty acids while $\Gamma_{f\to\ell}(g_{dw} \cdot m^{-3} \cdot min^{-1})$ is the rate at which they are converted into lipids (triacylglycerols). The latter one is assumed to depend in a linear fashion from the concentration of free fatty acids as well as from an additional saturation term that takes into account the decrease in oil production as cells become saturated with oil (Surisetty et al., 2010). Therefore, the mass balance for the lipidic fraction can be written as follows:

$$\frac{dC_\ell}{dt} = \Gamma_{f\to\ell} = k_{f\to\ell} \cdot C_f \cdot \left(1 - \frac{q_\ell}{q_\ell^{max}}\right) \tag{13}$$

along with the corresponding initial condition:

$$C_\ell = q_\ell^0 C_b^0 \quad at \quad t = 0 \tag{14}$$

where q_ℓ is the lipid cell quota which can be evaluated at each cultivation time as $q_\ell = C_\ell/C_b$, being C_b the total biomass concentration, i.e. the sum of the three compartment concentrations $C_b = C_\ell + C_f + C_x$.

3.4. Evaluation of light distribution and its effects on the chlorophyll's synthesis

Finally, in order to complete the set of equations of the model it should be specified that the term q_{Chla} in Eq. (1) represents the amount of chlorophyll-a (Chla) per unit of microalgal biomass, namely the chlorophyll cell quota ($g_{Chla} \cdot g_{dw}^{-1}$). In this regard, it is important to highlight that the Chla content of algae change as a result of photo-acclimation phenomena. Specifically, as the light intensity (I_{av}) in the culture decreases due to the increase of medium optical density, the algal cell is capable to synthesize "ex novo" new photosynthetic units (PSUs), containing chlorophyll-a, in order to better capture the incident photons (Strzepek et al., 2012). This acclimation mechanism allows the algae to adapt pigment (and especially chlorophyll) synthesis to light intensity. Ultimately, in order to acclimate to the low light conditions, microalgae utilize a certain fraction of the assimilated nitrogen for synthesizing new molecules of Chla. Consequently, the synthesis rate of chlorophyll-a is strictly linked to the nitrogen uptake rate (v_N) and thus the mass balance for the chlorophyll cell quota can be then written as follows:

$$\frac{dq_{Chla}}{dt} = \theta_{Chla}^N \cdot v_N - \mu \cdot q_{Chla} \tag{15}$$

along with the initial condition:

$$q_{Chla} = q_{Chla}^0 \quad at \quad t = 0 \tag{16}$$

where $\theta_{Chla}^N(g_{Chla} \cdot g_{dw}^{-1})$ is the amount of chlorophyll-a synthesized for every weight unit of nitrogen assimilated by algae. In the light of what above, θ_{Chla}^N depends upon light intensity as follows (Ward et al., 2012):

$$\theta_{Chla}^N = \theta_{Chla}^{N,max} \cdot \left(\frac{P}{\alpha \cdot \Phi \cdot q_{Chla} \cdot I_{av}}\right) \tag{17}$$

where $\theta_{Chla}^{N,max}$ Z is the maximum ratio at which nitrogen can be used for chlorophyll synthesis. In order to evaluate the average light intensity (I_{av}) within the culture, the following equation has been considered (Concas et al., 2016):

$$I_{av}(t) = \frac{2 \cdot I_0(t)}{R \cdot \tau_a \cdot C_b(t) \cdot \pi}\left[1 - \int_0^{\frac{\pi}{2}} \cos(\omega) \cdot \exp(-2 \cdot R \cdot \tau_a \cdot C_b(t) \cdot \cos(\omega)) \cdot d\omega\right] \tag{18}$$

where the symbol significance is reported in the Notation. The incident light intensity $I_0(t)$ appearing in Eq. (18), which varies with

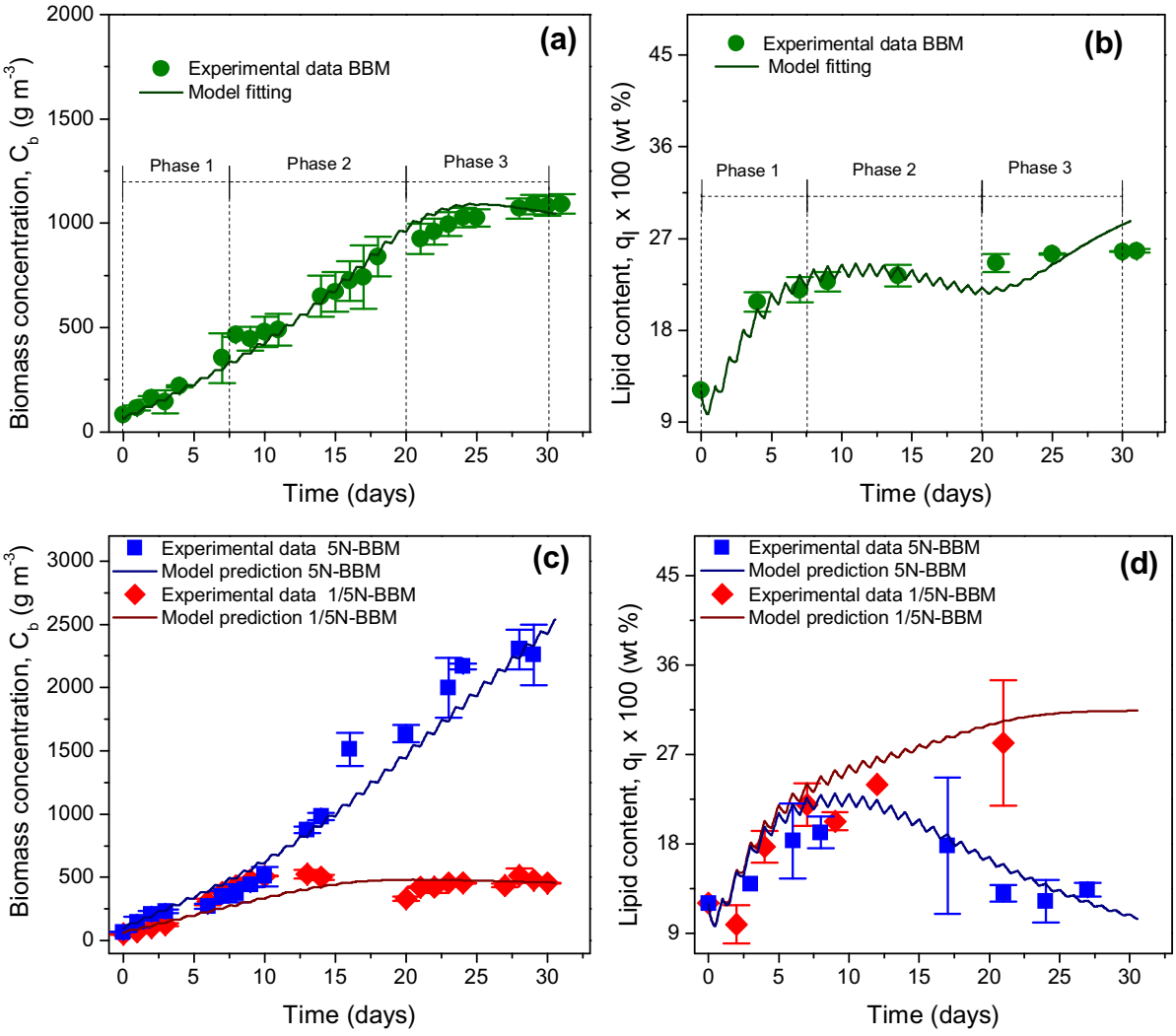

Fig. 2. Comparison between model results (fitting and prediction) and experimental data in terms of evolution in time of total biomass concentration (a and c), and in terms of lipid content (b and d) of microalgae when varying the initial concentration of nitrogen in solution.

time as a square wave having amplitude equal to 100 μE m^{-2} s^{-1} and a photoperiod equal to 12 h, is evaluated according to the method proposed by Concas et al., (2014b).

3.5. Mathematical modeling of the BIOCOIL photobioreactor

In order to quantitatively interpret the experimental results obtained with the BIOCOIL, through the present model, the following considerations have been made. During cultivation, the culture was entirely recirculated in the BIOCOIL and thus, from a macroscopic point of view the reactor was operated in the batch mode. Thus, the same equations so far presented, hold true for the simulation of growth and lipid production in the BIOCOIL with the exception that the reactor radius R in Eq. (18) coincides in this case with the radius of the tube of the coil, which is equal to 1 cm. Furthermore, to simulate the fed batch operation of the BIOCOIL occurring after 14 days of cultivation, the following equations were adopted instead of the Eqs. (4), (8), (11) and (13) respectively.

$$\frac{dC_N}{dt} = -v_N \cdot C_x + D \cdot (C_N^0 - C_N) \tag{19}$$

$$\frac{dC_x}{dt} = (\mu - k_d - D) \cdot C_x \tag{20}$$

$$\frac{dC_f}{dt} = \frac{(P - \gamma_{c/x}\mu)C_x}{\gamma_{c/f}} - \Gamma_{f\to\ell} - D \cdot C_f \tag{21}$$

$$\frac{dC_\ell}{dt} = k_{f\to\ell} \cdot C_f \cdot \left(1 - \frac{q_\ell}{q_\ell^{\max}}\right) - D \cdot C_\ell \tag{22}$$

along with the same corresponding initial conditions reported in the Eqs. (5), (9), (12) and (14) respectively. The symbol D(min^{-1}) represents the dilution ratio adopted during the fed batch cultivation of the reactor.

3.6. Numerical methods adopted for solving the mathematical model

The proposed mathematical models consists of a system of ordinary differential equations which was numerically integrated as an initial value problem with the Gear method by means of the subroutine DIVPAG of the standard numerical libraries (IMSL), while the integral of Eq. (18) was solved by invoking the IMSL subroutine DQDAWO. Tuning of model parameters values to fit the experimental data was carried out through an optimization procedure which minimize an objective function by means of the Fortran subroutine BURENL (Manca and Buzzi-Ferraris, 1996) based on the least-squares method.

Table 1
Model parameters.

Symbol	Value	Units	References
C_b^0	65.0 ÷ 95.0	$g_{dw}\ m^{-3}$	Experimentally evaluated
K_N	19.00	$g_N\ m^{-3}$	Concas et al. (2014b)
P_c^{max}	$1.69 \cdot 10^{-3}$	$g_C\ g_{dw}^{-1}\ min^{-1}$	Falkowski et al. (1985) and MacIntyre et al. (2002)
Q_N^{max}	$7.70 \cdot 10^{-2}$	$g_N\ g_{dw}^{-1}$	Concas et al. (2014b) and Picardo et al. (2013)
Q_N^{min}	$4.76 \cdot 10^{-2}$	$g_N\ g_{dw}^{-1}$	Bougaran et al. (2010), Mairet et al. (2011) and Packer et al. (2011)*
k_d	$1.20 \cdot 10^{-5}$	min^{-1}	Edmundson and Huesemann (2015) and Richards and Mullins (2013)
$k_{f\to l}$	$3.00 \cdot 10^{-4}$	min^{-1}	This work
q_{Chla}^0	$1.20 \cdot 10^{-2}$	$g_{Chla}\ g_{dw}^{-1}$	Piorreck et al. (1984)
q_N^0	$7.10 \cdot 10^{-2}$	$g_N\ g_{dw}^{-1}$	Evaluated from Picardo et al. (2013)
q_ℓ^{max}	$3.10 \cdot 10^{-1}$	$g_{dw}\ g_{dw}^{-1}$	Evaluated as the max value observed in the experiments
q_ℓ^0	$1.21 \cdot 10^{-1}$	$g_{dw}\ g_{dw}^{-1}$	Experimentally evaluated
v_N^{max}	$4.02 \cdot 10^{-5}$	$g_N\ g_{dw}^{-1}\ min^{-1}$	Evaluated from Shriwastav et al. (2014)
α	$7.50 \cdot 10^{1}$	$m^2\ g_{Chla}^{-1}$	This work
$\gamma_{c/f}$	$7.60 \cdot 10^{-1}$	$g_C\ g_{dw}^{-1}$	Evaluated from experiments and Geider and La Roche (2002))
$\gamma_{c/x}$	$6.10 \cdot 10^{-1}$	$g_C\ g_{dw}^{-1}$	Packer et al. (2011)
$\theta_{Chla}^{N,max}$	$2.14 \cdot 10^{-1}$	$g_{Chla}\ g_N^{-1}$	Ward et al. (2012)
μ_{max}	$7.25 \cdot 10^{-4}$	min^{-1}	Kumar and Das (2012) and Picardo et al. (2013)*
τ_a	$4.35 \cdot 10^{-1}$	$m^2\ g^{-1}$	Concas et al. (2014b)
Φ	$1.20 \cdot 10^{-6}$	$g_C\ \mu E^{-1}$	Packer et al. (2011)

* Average between the values reported by the references.

4. Results and discussion

4.1. Results obtained with lab-scale PBRs

Specific experiments were carried out by cultivating *C. sorokiniana* in batch stirred bottles where the initial concentration of dissolved nitrogen was suitably changed. In particular, the growth and lipid accumulation kinetics occurring when using nitrogen concentration equal to the one of BBM, i.e. 41.6 $g_N m^{-3}$, was first investigated as base case. The obtained results are shown in Fig. 2a in terms of algal biomass concentration evolution. It can be observed that the culture starts growing almost exponentially, without a significant lag phase, until about 20 days when the decelerating growth takes place. After 22 days, the culture achieves a kind of "plateau" in correspondence of biomass concentration of about 1000 $g_{dw} m^{-3}$, as a result of the exhaustion of nutrients available in solution. The corresponding evolution of lipid content is shown in Fig. 2b. As it can be observed, by starting from an initial value of about 12%wt, the lipid content increases significantly during the first cultivation days achieving a value close to 20%wt after only 4 days. Subsequently, the lipid content keeps increasing, even if with a reduced rate, and attains the value of about 26%wt after 30 days of cultivation.

Both in Fig. 2a and b, the comparisons between experimental data and model results are also shown. The model parameters adopted to perform the simulation are reported in Table 1. It should be noted that all model parameters are taken from the literature except for the optical cross section of chlorophyll-a (α) and the kinetic rate constant ($k_{f\to\ell}$) of conversion of fatty acids into lipids, which have been suitably tuned through a nonlinear fitting procedure to quantitatively interpret the experimental data.

The relative error obtained by the fitting procedure is equal to 8% while the values of α and $k_{f\to\ell}$ result to be $7.5 \cdot 10^1\ m^2 g_{Chla}^{-1}$, and $3.0 \cdot 10^{-4}\ min^{-1}$, respectively. It should be noted that, to the best of our knowledge, the value of the optical cross section of Chl-a (α) is not available in the literature for the strain *C. sorokiniana*. On the other hand, the obtained value is consistent with the range of values proposed in the literature for the optical section of different strains (Méléder et al., 2013).

From Fig. 2a and b, it is worth noting that, in general, the proposed model quantitatively captures both the growth trend and the lipid accumulation dynamics. The "oscillating" behavior of model displayed in Fig. 2a is due to the fact that, in absence of light, photosynthesis does not take place and thus biomass concentration does not increase correspondingly. On the other hand, from Fig. 2b it can be observed that model results show a slightly different trend of lipid accumulation with respect to the one observed in experiments, especially in the period of time ranging from 15 to 20 days. The simulated behavior can be explained as follows. During the first cultivation period (cf. phase 1 in the Figures), the culture is nitrogen replete and, at the same time, the low optical density permits a high penetration of light in the culture and thus photosynthesis can take place very efficiently thus leading to a high carbon fixation rate (P). Therefore, even if nitrogen is present in solution at high concentration, the term P is so large that growth rate is nitrogen controlled (cf. Fig. 1a). Accordingly, the term $(P - \gamma_{c/x}\mu) \cdot C_x/\gamma_{c/f}$ is greater than zero and the fatty acids synthesis (and thus lipid production) takes place at a high rate according to Eqs. (11) and (13). This explains the fast rate at which lipids are synthesized during the first cultivation days. However, as the culture grows, the optical density is augmented and the growth becomes light limited (cf. Fig. 1b). As a consequence, the term $(P - \gamma_{c/x}\mu) \cdot C_x/\gamma_{c/f}$ tends to vanish and thus the fatty acid synthesis is correspondingly inhibited (cf. Fig. 1b). Accordingly, the lipid content of microalgae stops growing, achieves a kind of plateau, and even starts to slightly decrease in the period ranging from 15 to 21 days (cf. Fig. 2b). Nevertheless, as the culture grows further nitrogen consumption leads the culture to become nitrogen limited again to the point that the biomass concentration achieves a plateau when the dissolved nitrogen is consumed. Under these conditions, growth and lipid synthesis become decoupled and, since the growth rate μ becomes equal to zero while the term P is greater than zero (cf. Fig. 1c), the rate of fatty acids production $(P - \gamma_{c/x}\mu) \cdot C_x/\gamma_{c/f}$ starts growing again. Accordingly, the simulated lipid content increases significantly in the period ranging from 22 to 30 days (cf. Fig. 2b). In the last cultivation days, this simulated trend is slightly different from the one observed in the experiments since the real value of the minimum nitrogen quota (Q_N^{min}) is probably lower than the one taken from the literature. However, it can be stated that, in general the experimental behavior is well captured by the model even in terms of lipid synthesis dynamics.

Table 2
Fatty acid methyl esters profile of lipids extracted from the microalgae cultivated under the different nitrogen concentrations investigated.

Carbon n°	FAME	BBM (%wt)	5N-BBM (% wt)	1/5N-BBM (% wt)
C14:0	Myristic	0.58 ± 0.01	0.15 ± 0.22	–
C16:0	Palmitic	27.50 ± 0.62	11.05 ± 0.01	20.79 ± 2.79
C16:1	Palmitoleic	5.18 ± 2.15	3.28 ± 1.34	7.25 ± 0.11
C17:0	Heptadecanoic	0.23 ± 0.04	0.16 ± 0.01	–
C18:0	Stearic	3.77 ± 0.30	1.51 ± 0.01	4.52 ± 0.29
C18:1	Oleic	9.65 ± 0.61	6.00 ± 0.39	15.71 ± 2.22
C18:2	Linoleic	32.18 ± 1.25	30.09 ± 0.84	28.84 ± 3.80
C18:3	Linolenic	19.72 ± 1.53	47.33 ± 0.68	21.22 ± 9.29
C20:0	Arachidic	0.43 ± 0.10	–	1.42 ± 0.25
C20:4	Arachidonic	–	0.12 ± 0.12	–
C22:0	Behenic	0.18 ± 0.03	–	0.10 ± 0.15
C22:6	Docosahexaenoic	0.11 ± 0.04	0.09 ± 0.14	–
C24:0	Lignoceric	0.34 ± 0.08	0.18 ± 0.26	0.12 ± 0.16
–	Other PUFAS	0.12 ± 0.01	–	–

In order to confirm the model capabilities, further experiments were performed and simulated. In particular, the new experiments were performed by setting the initial concentration of dissolved nitrogen equal to 5 times the corresponding value in the BBM medium. The corresponding experimental results are those marked with the tag 5 N-BBM in Fig. 2c and d. It can be observed from Fig. 2c that, under such operating conditions the culture keeps growing during the whole investigated time interval. Consequently, the value of biomass concentration at the end of the experiment, i.e. 2500 $g_{dw}m^{-3}$, is more than doubled with respect to the one correspondingly achieved in the base case experiment. Such a behavior is due to the fact that microalgae can prevent the decrease of their nitrogen cell quota by taking advantage of nitrogen available in solution which allows the sustainment of microalgal growth for a prolonged period of time. As it can be observed from Fig. 2c, such experimental behavior is quite well predicted by the proposed model without adjusting any model parameter with respect to the values of Table 1. The evolution of lipid accumulation observed in the framework of the same experiment is shown in Fig. 2d. Likewise what happened during the experiment with the BBM medium, also in this case a significant increase of the lipid content can be detected in the first days of cultivation. In fact the lipid content passes from an initial value of 12 wt% to about 19–20 wt% after 10 days of cultivation. This is because, during the first cultivation days, the low optical density of the culture allows an effective penetration of light which in turn boosts the photosynthetic fixation rate of carbon (cf. Fig. 1a). However, as it can be seen from Fig. 2d, after 10 days the lipid content of microalgae starts to decrease due to the fact that the increased optical density of culture and the simultaneous high availability of nitrogen leads the culture to be light-limited and thus, according to Fig. 1b, all the fixed carbon is used to synthesize functional biomass (x) rather than fatty acids. Therefore, the concentration of fatty acids (C_f) and lipids (C_ℓ) stops growing while the functional biomass (C_x) keeps increasing. As a consequence, the lipid content q_ℓ, i.e. the ratio between C_ℓ and the total biomass $C_b = C_x + C_f + C_\ell$, decreases. As it can be observed, the model is capable to reproduce these phenomena and to predict the experimental data quite well without tuning any model parameter.

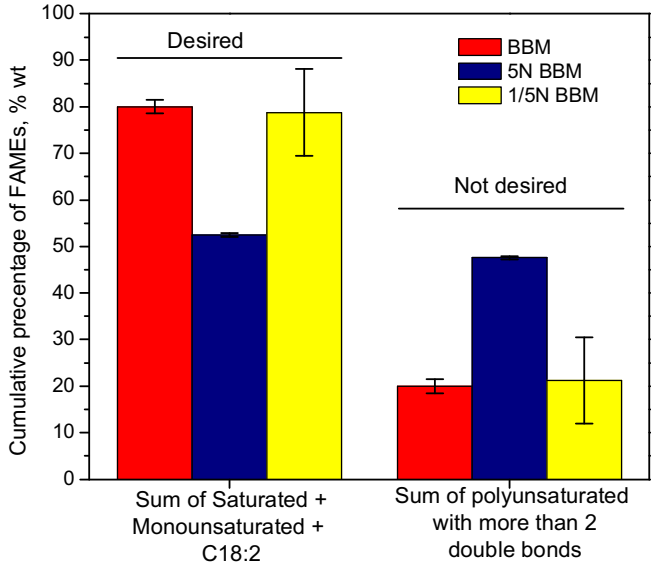

Fig. 3. Comparison between the cumulative weight percentages of macrocategories of FAMEs related to their usefulness for producing biodiesel and obtained under the investigated operating conditions.

In the Fig. 2c and d, the experimental results obtained when using an initial nitrogen concentration reduced by five times (1/5N-BBM) with respect to the one of the BBM medium, are also shown. In particular, as it can be appreciated from Fig. 2c, the culture achieves the steady state after about 10 days as a result of the consumption of nitrogen available in solution when the biomass concentration approaches a lower value of about 500 $g_{dw}m^{-3}$. On the contrary, the corresponding evolution of lipid shows a rowing trend for the entire investigated period of time (cf. Fig. 2d). In particular, when the nitrogen concentration in solution is reduced by five times the lipid accumulation dynamics in the first 15 days of cultivation is quite similar to the one already observed when cultivation was performed under the base case conditions or using 5N-BBM. However, after 15 days, i.e. when the biomass concentration achieves the steady state (cf. Fig. 2c), the corresponding lipid concentration greatly augments thus reaching quite high values, i.e. ~30%wt, at the 25th day of cultivation. This is since, when the biomass stops growing because of the achievement of the minimum nitrogen cell quota, all the carbon assimilated through photosynthesis is converted into fatty acids, and then into lipids, rather than into structural molecules. Therefore, when growth of biomass stops, lipids accumulate significantly within the cell. As it can be observed from the Fig. 2c and d, even in this case, the model well simulates the experimental results without tuning any parameter, thus confirming its predictive capability and reliability.

4.2. FAMEs obtained by transesterification of lipids produced in lab-scale PBRs

In order to verify whether the different cultivation conditions had affected the quality of microalgal lipids, the content of FAMEs was analyzed. It should be clarified that the FAMEs under concern are those obtained by transesterification of the lipids extracted from microalgae. The comparison among FAMEs profiles is reported in Table 2 in terms of weight percentage of each fatty acid with respect to the total amount of FAMEs identified. It can be observed that the FAMEs obtained from microalgae cultivated in the BBM medium showed a relatively high content of useful acids for producing biodiesel, i.e. palmitic (C16:0), linoleic (C18:2) and oleic acids (C18:1), even if a significant content of linolenic acid (C18:3) was detected. The latter one, in view of producing biodiesel, represents a counterproductive form of FAME due to its high instability under the action of light, temperature and oxygen and thus the lower its concentration the better is the potential biodiesel quality. Very similar FAMEs composition was obtained by transesterification of lipids extracted from microalgae cultivated under nitrogen starvation conditions (1/5N-BBM), even if in this case a slightly lower amount of linoleic acid and a slightly higher one of oleic acid (C18:1) were observed, respectively. By comparison, FAMEs obtained from microalgae cultivated under nitrogen excess (5N-BBM) displayed an higher content (~47%wt) of linolenic acid and thus were characterized by a lower suitability to produce biodiesel.

In order to get a quick idea about the effect of the initial nitrogen concentration on the suitability of the FAMEs for the production biodiesel, in Fig. 3 the aggregate amounts of fatty acids pertaining to the two macro categories "desired" and "undesired" are shown. Specifically the category "desired" takes into account the saturated fatty acids, the monounsaturated and linoleic acid while the "undesired" macro-category refers to the polyunsaturated ones with more than 2 double bonds. It can be observed that, with the view of producing biodiesel, the characteristics of oils extracted from microalgae grown in normal BBM and under nitrogen starvation conditions (1/5N-BBM) are quite similar since they have almost the same amounts of desired and undesired FAMEs,

respectively. On the contrary, the lipids extracted from microalgae grown in the nitrogen-rich growth medium (5N-BBM) are characterized by a significantly higher content of unsaturated fatty acids with more than two double bonds and thus are less suitable to be exploited for the production of biodiesel. Ultimately, while the biomass productivity of the culture grown in nitrogen-rich growth medium is quite high (cf. Fig. 2c), both the lipid content (cf. Fig. 2d) and its quality (cf. Fig. 3) are not satisfactory when compared to the corresponding ones obtained with the BBM and 1/5N-BBM medium. On the other hand, the lipids obtained when using the latter ones are quite similar both in terms of percent content and quality. However, since the biomass productivity obtained using the BBM medium is quite higher than the one obtained under nitrogen depletion, the former growth medium (i.e. the BBM) represents the optimal compromise between lipid productivity and quality achievable using *C. sorokiniana* grown under autotrophic conditions.

4.3. Results obtained with the BIOCOIL

For the reasons above, the BBM growth medium was used to perform the scale-up experiments in the BIOCOIL. In this regard, the evolution of biomass concentration during cultivation of *C. sorokiniana* in the BIOCOIL is shown in Fig. 4a. It can be observed that, such strain is capable to grow effectively in this photobioreactor showing a growth dynamics quite similar to the one already observed in the 1 L batch reactors, except for the seemingly lower value of biomass concentration achieved at the steady state. However, this lower biomass concentration is probably the result of the fed batch operation of the reactor starting from the 14th cultivation day. In fact, from that moment on, a culture volume of 800 mL was daily withdrawn from the reactor and then replaced by an equal volume of fresh BBM medium. The slight oscillations of experimental data noticeable around the value of about 900 ($g\,m^{-3}$) are just the result of this operation mode. Indeed, after each withdrawal, the biomass concentration first decreases and then re-starts growing due to the higher nutrient availability deriving from the fresh medium addition. The seeming steady state is slightly different from the one achieved in the corresponding batch experiments (cf. Fig. 2a) just because the fed-batch operation mode was started before the real steady state could be achieved in the BIOCOIL. According to the results shown in Fig. 2a, the steady state should be achieved at biomass concentration of about 1000 $g_{dw}m^{-3}$ while in this case the fed batch operation was started when the culture reached biomass concentration of about 900 $g_{dw}m^{-3}$. Apart from this aspect, the observed growth in the BIOCOIL demonstrates that the photobioreactor can be suitably operated in fed-batch mode using a dilution ratio of about 0.133 day^{-1} while ensuring the culture stability for very prolonged periods of time. As it can be observed from Fig. 4a, the corresponding experimental results are well predicted by the proposed model even when considering the fed-batch operation mode of the reactor. The saw-tooth trend of model results after the 14th day are due to the simulation of this operation mode. The dynamic evolution of lipid content during growth within the BIOCOIL is shown in Fig. 4b. Also in this case the evolution of the lipid accumulation is relatively similar to the one already observed in the small-scale reactors even if, overall, smaller lipid contents are achieved in the BIOCOIL. In fact, starting from an initial value of about 12%wt, the lipid content significantly grows during the first 5 days of cultivation reaching a value close to 23%wt. Subsequently the lipid accumulation occurs with a slower rate until the value of about 25%wt is achieved at the 35th day of cultivation. Such slight difference with the corresponding results obtained in the batch reactor, might be due to the fact that, while the oxygen developed by photosynthesis could be released from the liquid phase in the small batch reactor while the medium is pressurized in the tubes of the BIOCOIL and thus the photosynthetic oxygen is accumulated in the liquid phase, as growth proceeds. However, it is well known that, at high concentration, dissolved oxygen can damage the photosystem II of microalgae, thus reducing the capability of photosynthesis to fix the carbon that is subsequently converted into lipids. Moreover, the high concentration of oxygen might trigger lipid peroxidation phenomena (Concas et al., 2015), thus leading to a lower lipid content of microalgae. On the other hand, the observed reduction of lipid content might be due to the different reactor geometry and the resulting illumination conditions achieved in the BIOCOIL. Nevertheless, all these assumptions about the reduction of lipid content should be confirmed by focused experiments. In Fig. 4b, the comparison between experimental data and model predictions, is also shown. As it can be observed, while the general trend of lipid content evolution is enough well captured by the model, the

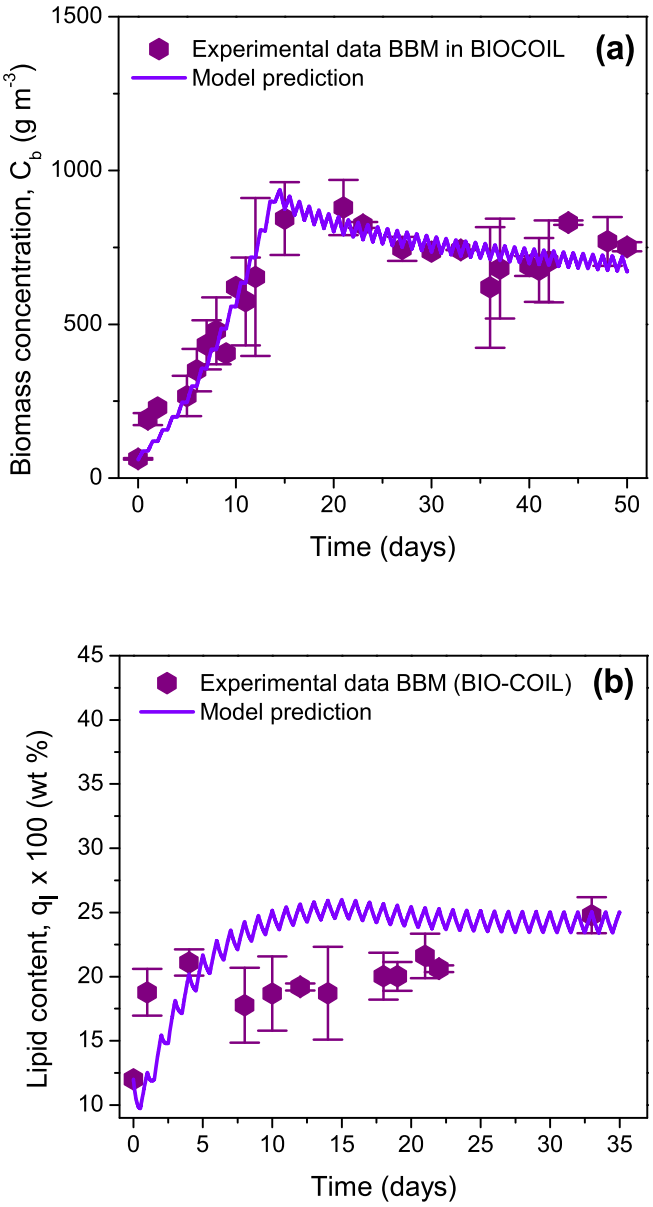

Fig. 4. Comparison between model results (predictions) and experimental data in terms of evolution in time of total biomass concentration (a) and lipid content (b) of microalgae when cultivated in the BIOCOIL photobioreactor using an initial nitrogen concentration equal to the one the BBM growth medium, i.e. 41.16 $g\,m^{-3}$.

experimental data regarding the period of time ranging from 5 to 20 days are over-estimated by the proposed model probably due to the fact that the latter one neglects the potential lipid oxidation phenomena discussed above. However, in general terms, it can be stated that even with reference to the lipid accumulation dynamics, the results obtained in the laboratory photobioreactors are well reproduced in the BIOCOIL, thus confirming the scalability of the obtained results also in terms of lipid productivity. Moreover, the proposed model, which should be any way improved, might be used in its present form to get an idea about the scale-up of the experimental results obtained at the laboratory level and thus for the optimization of the design and the set-up of BIOCOIL reactors.

An example of how the model might be used to identify the operating conditions which allow optimizing the BIOCOIL's productivities is shown in Fig. 5, where modeling results are reported in the form of contour maps showing the values of the

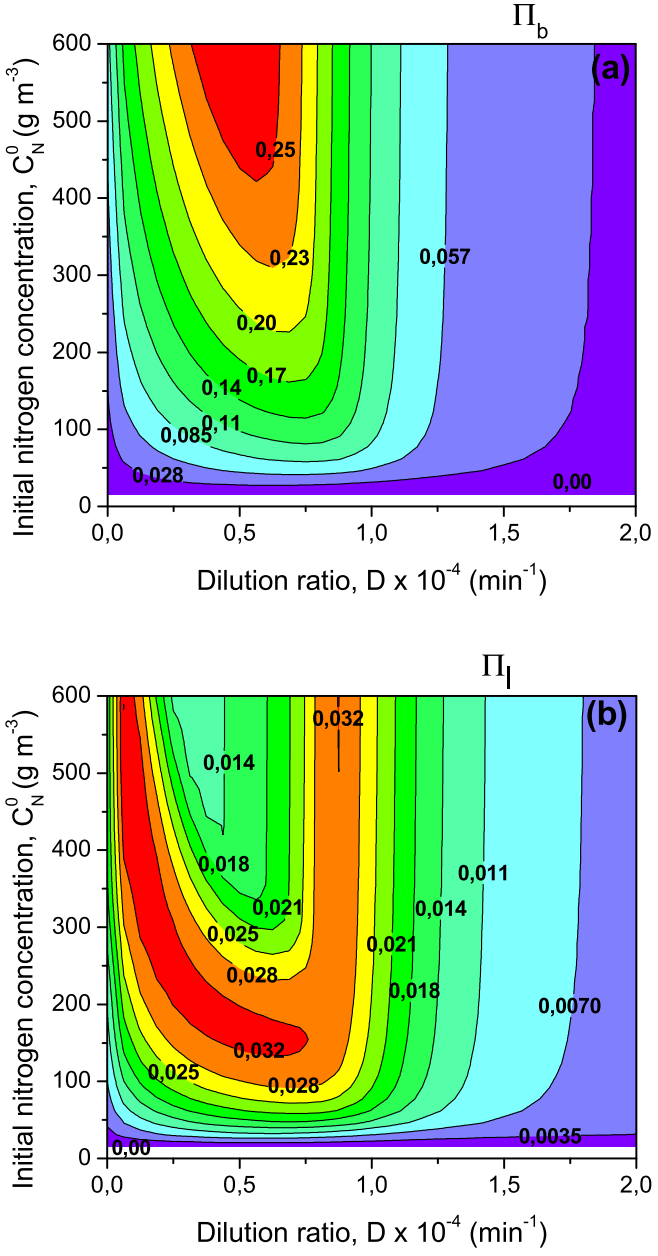

Fig. 5. Simulated optimization maps of (a) biomass ($g\ m^{-3}\ min^{-1}$) and (b) lipid productivities ($g\ m^{-3}\ min^{-1}$) achievable by operating the BIOCOIL photobioreactor in fed-batch mode starting from the 35th to the 75th day of cultivation, while using different values of initial nitrogen concentration as well as different dilution ratios.

average biomass and lipid productivities obtained by performing several simulations with different couples of values of initial concentrations of nitrogen C_N^0 and dilution rate D. The average productivities in terms biomass $\overline{\Pi}_b(gm^{-3}min^{-1})$ and lipid $\overline{\Pi}_\ell(gm^{-3}min^{-1})$ were evaluated, respectively, according to the following equations by assuming that the reactor was operated in the fed-batch mode starting from $t_i = 15(day)$ until $t_f = 75(day)$ day of cultivation, i.e. for two months, and then discharged at $t = t_f$:

$$\overline{\Pi}_b = \frac{\int_{t_i}^{t_f} D \cdot C_b(t) \cdot dt + C_b(t_f)}{t_f - t_i} \tag{23}$$

$$\overline{\Pi}_\ell = \frac{\int_{t_i}^{t_f} D \cdot C_\ell(t) \cdot dt + C_\ell(t_f)}{t_f - t_i} \tag{24}$$

As it can be observed, the optimization maps of Fig. 5 would allow one to suitably choose the value of the dilution ratio and of the initial concentration of nitrogen which result in the achievement of the optimal productivity in terms of biomass or lipids. In particular the maximum simulated lipid productivity, in this case, was equal to about 0.032 $gm^{-3}min^{-1}$ (cfr. region colored in red in Fig. 5b) and could be achieved through different couples of values of C_N^0 and D. This productivity value is quite good with respect to the average values of lipid productivity reported in the literature (Concas et al., 2014a). Such kind of tool would permit also to reduce the costs of nitrogen-based nutrients since, as it can be seen from the Figure, it shows that over a certain concentration of dissolved nitrogen there are no improvements in the resulting lipid productivity (cf. Fig. 5b). Therefore, the use of too high concentration of dissolved nitrogen as well as unsuitable dilution ratios might be potentially avoided by using the proposed mathematical model.

4.4. FAMEs obtained by transesterification of lipids produced in the BIOCOIL

Finally, in Fig. 6 the FAMEs profile of the oil extracted from the biomass grown in the BIOCOIL and then subjected to transesterification, is shown. By comparing the obtained results with the ones correspondingly achieved in the small batch reactor (cf. Table 2), no significant differences arise apart for a slight improvement of the quality of the oil. In fact, it can be observed from Fig. 6 that the main components are the linoleic (34%wt) and palmitic

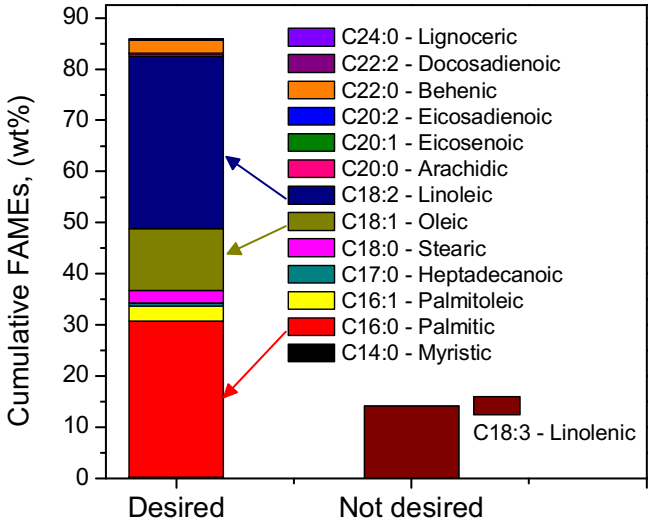

Fig. 6. Composition of FAMEs obtained through transesterification of lipids extracted from *C. sorkiniana* cultivated in the BIOCOIL photobioreactor.

(30.5%wt) acids which involve together the 63%wt of all the FAMEs. In this case the linolenic acid content is about 14%wt which, alone, represents all the "undesired" category of FAMES. Overall, the desired forms of FAMEs is of about 86 wt% while in the small photobioreactors the corresponding FAMEs amounted was of about 80 %wt in the best of the cases investigated. Therefore, from the qualitative point of view it can be stated that a slight improvement of the oil quality is achieved by cultivating *C. sorokiniana* in the BIOCOIL. However, the linolenic acid content is still slightly greater (14%wt) with respect to the maximum threshold (12%wt) imposed by European regulation for the quality biodiesel (EN 14103). For this reason, in order to be suitably exploited, the biodiesel obtained from *C. sorokiniana* should be subjected to a hydrogenation post-treatment. On the other hand, suitable techniques capable to reduce the amount of unsaturated FAMES, during the lipid extraction process itself, are currently under investigation along these lines.

5. Conclusions

A mathematical model for the simulation of the effect of nitrates on the batch growth and lipid accumulation of *C. sorokiniana*, is proposed. By comparing model results with experimental data a good matching is obtained. The model has been then successfully used to entirely predict the experimental results related to the growth in a BIOCOIL photobioreactor operated at a higher scale in fed-batch mode. The model thus permits to develop suitable optimization maps for the scale-up of the BIOCOIL. The FAMEs composition of lipids extracted from *C. sorokinina* is very close to the value which permits the production of biodiesel without a suitable pre-treatment.

Acknowledgements

The financial support of the Bio-Pilot INNOVARE project (Regione Autonoma della Sardegna, Italy) is gratefully acknowledged. One of us, C.C. acknowledges the financial support obtained from the University of Cagliari during her PhD program in environmental science and Engineering and his Assegno di Ricerca, respectively.

Appendix A. Supplementary data

Supplementary data associated with this article can be found, in the online version, at http://dx.doi.org/10.1016/j.biortech.2016.03.089.

References

Bougaran, G., Bernard, O., Sciandra, A., 2010. Modeling continuous cultures of microalgae colimited by nitrogen and phosphorus. J. Theor. Biol. 265, 443–454.
Cherif, M., Loreau, M., 2010. Towards a more biologically realistic use of Droop's equations to model growth under multiple nutrient limitation. Oikos 119, 897–907.
Concas, A., Pisu, M., Cao, G., 2016. A novel mathematical model to simulate the size-structured growth of microalgae strains dividing by multiple fission. Chem. Eng. J. 287, 252–268.
Concas, A., Pisu, M., Cao, G., 2015. Disruption of microalgal cells for lipid extraction through Fenton reaction: modeling of experiments and remarks on its effect on lipids composition. Chem. Eng. J. 263, 392–401.
Concas, A., Pisu, M., Cao, G., 2014a. Engineering Aspects Related to the Use of Microalgae for Biofuel Production and CO_2 Capture from Flue Gases. Current Environmental Issues and Challenges. Springer, pp. 73–111.
Concas, A., Steriti, A., Pisu, M., Cao, G., 2014b. Comprehensive modeling and investigation of the effect of iron on the growth rate and lipid accumulation of *Chlorella vulgaris* cultured in batch photobioreactors. Bioresour. Technol. 153, 340–350.
Edmundson, S.J., Huesemann, M.H., 2015. The dark side of algae cultivation: characterizing night biomass loss in three photosynthetic algae, *Chlorella sorokiniana*, *Nannochloropsis salina* and *Picochlorum* sp. Algal Res. 12, 470–476.
Fajardo, A.R., Cerdan, L.E., Medina, A.R., Fernández, F.G.A., Moreno, P.A.G., Grima, E. M., 2007. Lipid extraction from the microalga *Phaeodactylum tricornutum*. Eur. J. Lipid Sci. Technol. 109, 120–126.
Falkowski, P.G., Dubinsky, Z., Wyman, K., 1985. Growth-irradiance relationships in phytoplankton1. Limnol. Oceanogr. 30, 311–321.
Geider, R., La Roche, J., 2002. Redfield revisited: variability of C:N:P in marine microalgae and its biochemical basis. Eur. J. Phycol. 37, 1–17.
Klofutar, B., Golob, J., Likozar, B., Klofutar, C., Žagar, E., Poljanšek, I., 2010. The transesterification of rapeseed and waste sunflower oils: mass-transfer and kinetics in a laboratory batch reactor and in an industrial-scale reactor/separator setup. Bioresour. Technol. 101, 3333–3344.
Kobayashi, N., Barnes, A., Jensen, T., Noel, E., Andlay, G., Rosenberg, J.N., Betenbaugh, M.J., Guarnieri, M.T., Oyler, G.A., 2015. Comparison of biomass and lipid production under ambient carbon dioxide vigorous aeration and 3% carbon dioxide condition among the lead candidate Chlorella strains screened by various photobioreactor scales. Bioresour. Technol. 198, 246–255.
Kumar, K., Das, D., 2012. Growth characteristics of *Chlorella sorokiniana* in airlift and bubble column photobioreactors. Bioresour. Technol. 116, 307–313.
Likozar, B., Levec, J., 2014. Effect of process conditions on equilibrium, reaction kinetics and mass transfer for triglyceride transesterification to biodiesel: experimental and modeling based on fatty acid composition. Fuel Process. Technol. 122, 30–41.
MacIntyre, H.L., Kana, T.M., Anning, T., Geider, R.J., 2002. Photoacclimation of photosynthesis irradiance response curves and photosynthetic pigments in microalgae and cyanobacteria1. J. Phycol. 38, 17–38.
Mairet, F., Bernard, O., Masci, P., Lacour, T., Sciandra, A., 2011. Modelling neutral lipid production by the microalga *Isochrysis aff. galbana* under nitrogen limitation. Bioresour. Technol. 102, 142–149.
Manca, D., Buzzi-Ferraris, G., 1996. BurenI: a statistical package to calculate the values of parameters involved in a mathematical model. Dep. Chem. Eng. Politec.
Méléder, V., Laviale, M., Jesus, B., Mouget, J.L., Lavaud, J., Kazemipour, F., Launeau, P., Barillé, L., 2013. In vivo estimation of pigment composition and optical absorption cross-section by spectroradiometry in four aquatic photosynthetic micro-organisms. J. Photochem. Photobiol. B Biol. 129, 115–124.
Mishra, S.K., Suh, W.I., Farooq, W., Moon, M., Shrivastav, A., Park, M.S., Yang, J.-W., 2014. Rapid quantification of microalgal lipids in aqueous medium by a simple colorimetric method. Bioresour. Technol. 155, 330–333.
Negi, S., Barry, A.N., Friedland, N., Sudasinghe, N., Subramanian, S., Pieris, S., Holguin, F.O., Dungan, B., Schaub, T., Sayre, R., 2015. Impact of nitrogen limitation on biomass, photosynthesis, and lipid accumulation in *Chlorella sorokiniana*. J. Appl. Phycol., 1–10
Orsini, M., Cusano, R., Costelli, C., Malavasi, V., Concas, A., Angius, A., Cao, G., 2016a. Complete genome sequence of chloroplast DNA (cpDNA) of *Chlorella sorokiniana*. Mitochondrial DNA 27, 1539–1541.
Orsini, M., Cusano, R., Costelli, C., Malavasi, V., Concas, A., Angius, A., Cao, G., 2016b. Complete genome sequence of chloroplast DNA (cpDNA) of Chlorella sorokiniana. Mitochondrial DNA 27, 838–839.
Packer, A., Li, Y., Andersen, T., Hu, Q., Kuang, Y., Sommerfeld, M., 2011. Growth and neutral lipid synthesis in green microalgae: a mathematical model. Bioresour. Technol. 102, 111–117.
Picardo, M.C., de Medeiros, J.L., Monteiro, J.G.M., Chaloub, R.M., Giordano, M., de Araújo, O.Q.F., 2013. A methodology for screening of microalgae as a decision making tool for energy and green chemical process applications. Clean Technol. Environ. Policy 15, 275–291.
Piorreck, M., Baasch, K.-H., Pohl, P., 1984. Biomass production, total protein, chlorophylls, lipids and fatty acids of freshwater green and blue-green algae under different nitrogen regimes. Phytochemistry 23, 207–216.
Quinn, J., De Winter, L., Bradley, T., 2011. Microalgae bulk growth model with application to industrial scale systems. Bioresour. Technol. 102, 5083–5092.
Richards, R.G., Mullins, B.J., 2013. Using microalgae for combined lipid production and heavy metal removal from leachate. Ecol. Model. 249, 59–67.
Sharma, K.K., Schuhmann, H., Schenk, P.M., 2012. High lipid induction in microalgae for biodiesel production. Energies 5, 1532–1553.
Shriwastav, A., Gupta, S.K., Ansari, F.A., Rawat, I., Bux, F., 2014. Adaptability of growth and nutrient uptake potential of *Chlorella sorokiniana* with variable nutrient loading. Bioresour. Technol. 174, 60–66.
Šoštarič, M., Klinar, D., Bricelj, M., Golob, J., Berovič, M., Likozar, B., 2012. Growth, lipid extraction and thermal degradation of the microalga *Chlorella vulgaris*. N. Biotechnol. 29, 325–331.
Steriti, A., Rossi, R., Concas, A., Cao, G., 2014. A novel cell disruption technique to enhance lipid extraction from microalgae. Bioresour. Technol. 164, 70–77.
Strzepek, R.F., Hunter, K.A., Frew, R.D., Harrison, P.J., Boyd, P.W., 2012. Iron-light interactions differ in Southern Ocean phytoplankton. Limnol. Oceanogr. 57, 1182–1200.
Surisetty, K., la Hoz Siegler, H., McCaffrey, W.C., Ben-Zvi, A., 2010. Model re-parameterization and output prediction for a bioreactor system. Chem. Eng. Sci. 65, 4535–4547.
Ward, B.A., Dutkiewicz, S., Jahn, O., Follows, M.J., 2012. A size-structured food-web model for the global ocean. Limnol. Oceanogr. 57, 1877.